AIP | Applied Physics Letters

Focusing guided waves using surface bonded elastic metamaterials

Xiang Yan, Rui Zhu, Guoliang Huang, and Fuh-Gwo Yuan

Citation: Appl. Phys. Lett. **103**, 121901 (2013); doi: 10.1063/1.4821258
View online: http://dx.doi.org/10.1063/1.4821258
View Table of Contents: http://apl.aip.org/resource/1/APPLAB/v103/i12
Published by the AIP Publishing LLC.

Focusing guided waves using surface bonded elastic metamaterials

Xiang Yan,[1] Rui Zhu,[2] Guoliang Huang,[2] and Fuh-Gwo Yuan[1,a)]
[1]*Department of Mechanical and Aerospace Engineering, North Carolina State University, Raleigh, North Carolina 27695, USA*
[2]*Department of Systems Engineering, University of Arkansas at Little Rock, Little Rock, Arkansas 72204, USA*

(Received 8 June 2013; accepted 25 August 2013; published online 16 September 2013)

Bonding a two-dimensional planar array of small lead discs on an aluminum plate with silicone rubber is shown numerically to focus low-frequency flexural guided waves. The "effective mass density profile" of this type of elastic metamaterials (EMMs), perpendicular to wave propagation direction, is carefully tailored and designed, which allows rays of flexural A_0 mode Lamb waves to bend in succession and then focus through a 7×9 planar array. Numerical simulations show that Lamb waves can be focused beyond EMMs region with amplified displacement and yet largely retained narrow banded waveform, which may have potential application in structural health monitoring. © *2013 AIP Publishing LLC*. [http://dx.doi.org/10.1063/1.4821258]

Lamb waves are transient elastic waves traveling in plate-like structures guided by two parallel free surfaces. The wave dispersion in a lossless elastic medium is a consequence of a wave interference phenomenon, rather than a physical property of the material. As a result, Lamb waveforms will be distorted and further attenuated in amplitude due to geometry spreading as the propagation distance (or time duration) increases. The Lamb wave based structural health monitoring (SHM) methods have been attracting much attention mainly due to their capability of long-range and through-the-thickness interrogation of the structures. In a common Lamb wave based SHM test setup for damage detection, omnidirectional circular piezoelectric wafers are often used to excite and sense the wave signals. However, the sensed signals are often not easy to interpret due to the low signal-to-noise ratio (SNR) caused by dispersion[1] and ambient environments. To increase the SNR for detecting damage in high resolution, focusing Lamb waves that propagating with different paths emitted from an array of piezoelectric transducers with different time delays at the sensor location where defects might occur have been proven to be effective.[1–3]

Recently, focusing of the lowest flexural (or antisymmetric) Lamb wave in a perforated gradient-index (GRIN) phononic crystal (PC) plate was demonstrated numerically by Wu *et al.*[4] and was reported both numerically and experimentally by Zhao *et al.*[5] The inherent Bragg scattering mechanism[6] of PC usually requires the dimension of the microstructure unit cell comparable with the manipulated wavelength, which makes it unsuitable for relative low frequency application such as SHM. In addition, to detect the damage in structures using SHM techniques, using this approach by degrading the strength of the pristine structure through perforation is strictly prohibitive in SHM.

With the rapid development of electromagnetic metamaterials, the principle of metamaterial has been extended to acoustic and elastic media very recently. Acoustic/elastic metamaterials (AMMs/EMMs) are engineered composites, usually through structure design, to exhibit unusual effective properties under external stimulus.[7] Various schemes for AMMs/EMMs have been proposed to realize negative effective properties.[8–10] The intrinsic mechanism of EMM is the local resonance, while the inherent Bragg scattering is attributed to mechanism of PC.[6] This primary difference has made the distinct energy dissipation mechanism between EMM and PC. For EMM, the wave energy dissipated in the resonators in form of kinetic energy, while for PC the wave dissipation is mainly caused by the multiple scattering, which will be much lower than the EMM. However, since each EMM contains its local resonance, focusing Lamb waves using EMMs in relatively low frequency that can be used in SHM becomes a reality. Therefore, by the use of the positive effective property of EMMs, an EMM plate design by bonding small-sized structures with varying positive effective mass densities which can both maintain the strength of the host structure with slight weight penalty and at the same time achieve focusing under relatively lower working frequency is very preferable.

In this letter, a design of surface-bonded EMMs is proposed to achieve effective mass density profile and focus ultrasonic Lamb waves in an aluminum plate. It is shown that Lamb waves can be focused outside the EMM region in relatively low ultrasonic frequency range, and amplified wave signals which still largely retain the original waveform are observed at focal spot and its surrounding area. The EMMs considered in this study consist of lead discs with varying thicknesses bonded on an aluminum plate using uniform thickness silicone rubber.[11] One cell of EMM plate is shown in Figure 1.

It has been known in optics (e.g., Gomez-Reino *et al.*[12]) that the light beam can be focused and defocused in a smoothly gradient-index media with the refractive index varying around the optical axis. Lin *et al.*[13] recently proposed a refractive index profile in the form of a hyperbolic secant which enables acoustic wave focusing inspired from the light beam focusing. Wu *et al.*[4] and Zhao *et al.*[5] conceptualized PC to achieve Lamb waves focusing in perforated silicone plate using the same hyperbolic refractive index

a)Author to whom correspondence should be addressed. Electronic mail: yuan@ncsu.edu

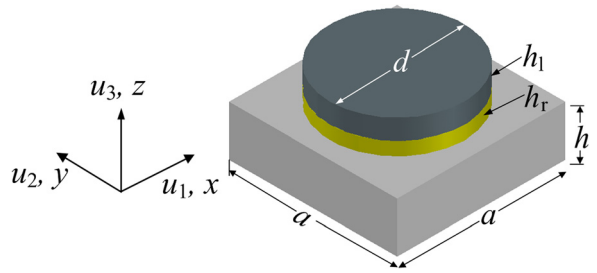

FIG. 1. One cell of EMM plate.

profile, and they defined the refractive index as the ratio of the group velocity in the homogenous plate and the perforated plate. The proposed EMMs plate for Lamb waves focusing is to vary effective mass densities that can be tailored from different EMM cells. As Lamb waves propagate within two EMM cells having varying effective mass densities, wave propagation direction will be bent due to the change of phase velocity. The goal of this letter is to design an effective mass density profile using surface bonded EMMs perpendicular to the direction of wave propagation to focus a narrow banded A_0 mode Lamb waves (center frequency: 30 kHz) which may be useful in future SHM. An effective out-of-plane mass density profile in the form of a hyperbolic secant is proposed to achieve the A_0 mode Lamb waves focusing

$$\rho_{\text{eff}}(y) = \rho_{\text{eff},0}\,\text{sech}^2(\alpha y), \tag{1}$$

where $\rho_{\text{eff},0}$ is the effective mass density of the reference cells in an array located at $y = 0$ and α gradient coefficient, characterizing the degree of focusing. Figure 2 shows the hyperbolic secant effective mass density profile. EMM cells with varying effective mass densities need to be designed and located at different y locations to best fit the profile. Varying effective mass densities can be tailored by only changing the height of lead disc (h_l) in each cell. Other geometrical parameters used in this study shown in Figure 1 are kept constant: $a = 5$ mm, $d = 4$ mm, $h = 1.5$ mm, and $h_r = 0.4$ mm.

A numerically based effective medium method[14] is adopted for determination of the out-of-plane effective mass density of the EMM cell. Under the assumption that the wavelengths corresponding to the prescribed ultrasonic frequency are much larger than the characteristic dimensions of the EMM cell, the out-of-plane effective mass density for this problem can be defined as $\rho_{\text{eff}} = F_3/\ddot{U}_3$, where F_3 and $\ddot{U}_3$ are the effective resultant force and acceleration of this

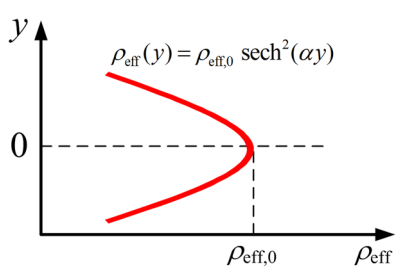

FIG. 2. Hyperbolic secant effective mass density profile.

cell on the external surrounding boundary. By imposing the time-harmonic displacement constraints $U_1 = U_2 = 0$, and $U_3 = Ae^{-i\omega t}$ on the external surrounding boundary, the effective mass density is calculated by

$$\rho_{\text{eff}} = -F_3/\omega^2 AV, \tag{2}$$

where V is the volume of the cell.

The effective mass density of the EMM cell is extracted from numerically based effective medium method using time-harmonic excitation. However, in a common Lamb wave based SHM test setup for damage detection, a narrowband five-peaked toneburst signal is often used for Lamb wave excitation from the piezoelectric actuator. The excitation voltage signal is governed by

$$V_{\text{in}}(t) = P[H(t) - H(t - N_p/f_c)] \times (1 - \cos(2\pi f_c t/N_p))\sin(2\pi f_c t), \tag{3}$$

where peak number $N_p = 5$, constant P is signal intensity, f_c is the center frequency, and $H(t)$ is a Heaviside step function. It can be seen through the frequency domain analysis (Figure 3) that the frequency components for this narrowband signal mainly concentrate in a small region around the center frequency $f_c = 30$ kHz. The corresponding wavelength is 21.7 mm. Since the transient excitation is a summation of different time-harmonic excitations, this narrowband transient five-peaked toneburst signal can be approximated as a 30 kHz harmonic excitation. The frequency dependent effective mass density plot of a reference cell ($h_l = 0.59$ mm) using numerical model is shown in Figure 3. From the figure, the resonant frequency of the reference cell is slightly greater than 30 kHz and its effective mass density under 30 kHz harmonic excitation is determined as $\rho_{\text{eff},0} = 62944\ \text{kg/m}^3$.

To minimize the weight penalty that exerts on the host aluminum plate, only five different EMM cells, one at the center and the other four pairs are placed symmetrically with respect to the reference cell as shown in Figure 5(a). Substituting $\rho_{\text{eff},0} = 62944\ \text{kg/m}^3$ and the gradient coefficient determined as $\alpha = 0.038\ \text{mm}^{-1}$ into Eq. (1), the effective mass

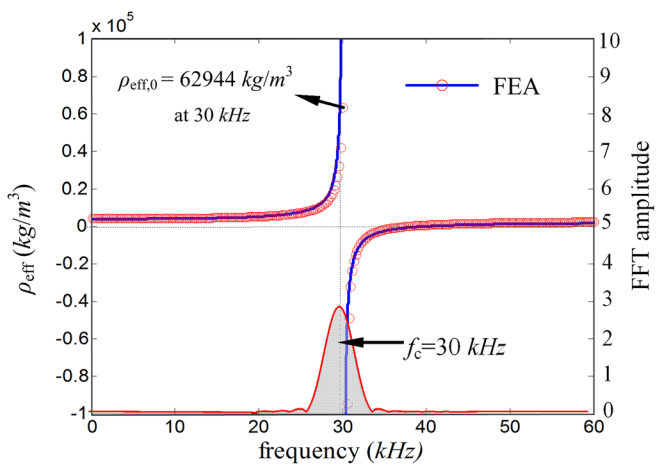

FIG. 3. Effective mass density-frequency plot and amplitude spectrum of the five-peaked Hanning windowed tone burst excitation signal centered at 30 kHz.

TABLE I. Lead disc height, resonant frequency, and effective mass density of each cell.

Cell number	y (mm)	h_1 (mm)	f_0 (kHz)	ρ_{eff} (kg/m^3) ($f_c = 30$ kHz)
0	0	0.590	30.2	62 944
1	±5	0.589	30.2	59 911
2	±10	0.586	30.4	52 359
3	±15	0.581	30.4	44 172
4	±20	0.572	30.6	35 043

densities of other four EMM cells are calculated as $\rho_{\text{eff}}(\pm 5\,\text{mm}) = 59911\,\text{kg/m}^3$, $\rho_{\text{eff}}(\pm 10\,\text{mm}) = 53858\,\text{kg/m}^3$, $\rho_{\text{eff}}(\pm 15\,\text{mm}) = 44790\,\text{kg/m}^3$, and $\rho_{\text{eff}}(\pm 20\,\text{mm}) = 35189\,\text{kg/m}^3$. Therefore, the four EMM cells with varying effective mass densities that can best fit the target effective mass densities are needed. These effective mass densities can then be obtained using the effective medium method by carefully changing the lead disc height so that the resonant frequency of each EMM cell is slightly greater than 30 kHz. The height of the lead disc, resonant frequency and effective mass density of different EMM cell are listed in Table I. With the planar array of surface-bonded EMMs having effective mass density profile, seven identical EMM horizontal arrays are placed equidistant along x direction with width 35 mm that is smaller than the focal length $f = \pi/2\alpha = 41.3$ mm. This assures that Lamb waves can be focused outside the EMMs region, shown in Figure 5(b).

To explore the A_0 mode focusing at 30 kHz, a 7×9 planar EMM array is bonded on the aluminum plate (600 mm × 400 mm × 1.5 mm) in parallel with the actuator at a distance of 120 mm and the rectangular shaped actuator (60 mm × 5 mm × 0.2 mm) is attached vertically on the location 280 mm away from the left edge of the plate. Figure 4 shows the 7×9 planar array of the aluminum plate with EMMs attached. The rectangular-shaped actuator is chosen to ensure a near planar wave front when Lamb waves propagate into the gradient index EMMs region. With the tactfully designed EMMs region having effective mass density profile, as Lamb waves propagate within different EMM cells, the waves behave like propagating from one material to another due to impedance mismatch. Therefore, wave propagation direction and velocity will deflect and change as they propagate through the boundaries of different EMM cells. The rays of Lamb

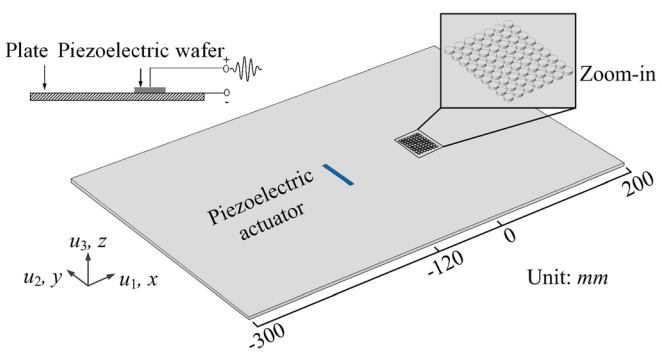

FIG. 4. Layout of EMMs plate with piezoelectric actuator.

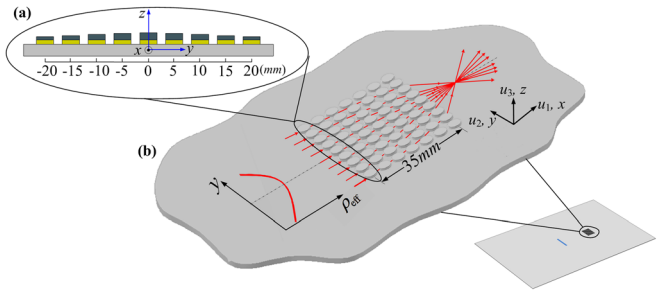

FIG. 5. (a) Close-up EMM array, (b) Close-up 7×9 planar EMM array region and trajectory of Lamb waves focusing.

waves will be bent in succession toward the center axis and focused to a local area on the aluminum plate as shown in Figure 5(b). Although the excitation signal is mainly concentrated at 30 kHz, there are still other frequency components (Figure 3) around 30 kHz. Therefore, it is expected that Lamb waves would be focused onto a wider focal region rather than a single spot, while the largest amplified displacement should still appear around the predicted focal spot corresponding to 30 kHz Lamb waves.

A finite element method (FEM) was adopted to simulate the 30 kHz A_0 wave mode through an aluminum plate with surface-bonded EMMs (Figure 4). Displacement contour in z direction at different time steps is used to observe focusing phenomenon. A nearly planar wave front is formed as the forward propagating waves travel into the EMMs region, shown in Figure 6(a). As the waves propagating inside the gradient index EMMs regions, Lamb waves are bent gradually toward the center axis. Figure 6(b) clearly shows the occurrence of convergence of Lamb waves with a bent wave front. By contrast, the backward propagating waves still maintain the near planar wave front. Figure 6(c) shows that the waves are focused to a focal spot (area) with the largest out-of-plane displacement as 0.3922 μm which is more than two times than the amplitude of the backward propagating waves without focusing due to dispersion. After the forward propagating waves travel past the EMMs, the waves start to diverge as shown in Figure 6(d). The focal spot appears around $x = 51$ mm, which is slightly deviated from the theoretical predicted one as $x = 46.4$ mm. The difference may arise from the imprecise determination of the gradient coefficient because it is difficult to precisely choose the effective mass densities to fit the exact hyperbolic secant profile. In addition, the slightly coupling of the S_0 mode Lamb wave might be another source that can affect focal lengths. Furthermore, Lamb waves propagating into EMMs region with imperfect planar wave front may be the other reason as well. The width of the EMMs region and the gradient coefficient α can be changed to focus Lamb waves to any arbitrary location of the plate.

In order to utilize the proposed EMMs Lamb waves focusing method in SHM, it is critical to examine the displacement response of the A_0 mode past through the EMMs region. Four locations on the center axis of the plate are chosen to investigate the out-of-plane displacement response after A_0 mode Lamb waves have progressed beyond the EMM

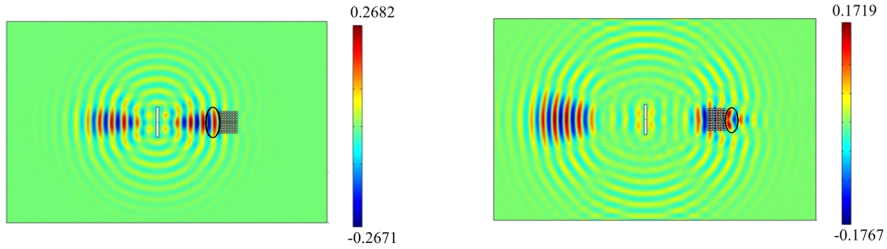

(a) Displacement contour in z direction at $t = 140\ \mu s$ (b) Displacement contour in z direction at $t = 197\ \mu s$

(c) Displacement contour in z direction at $t = 259\ \mu s$ (d) Displacement contour in z direction at $t = 290\ \mu s$

FIG. 6. Snapshots of out-of-plane displacement contour (μm) for Lamb waves focusing.

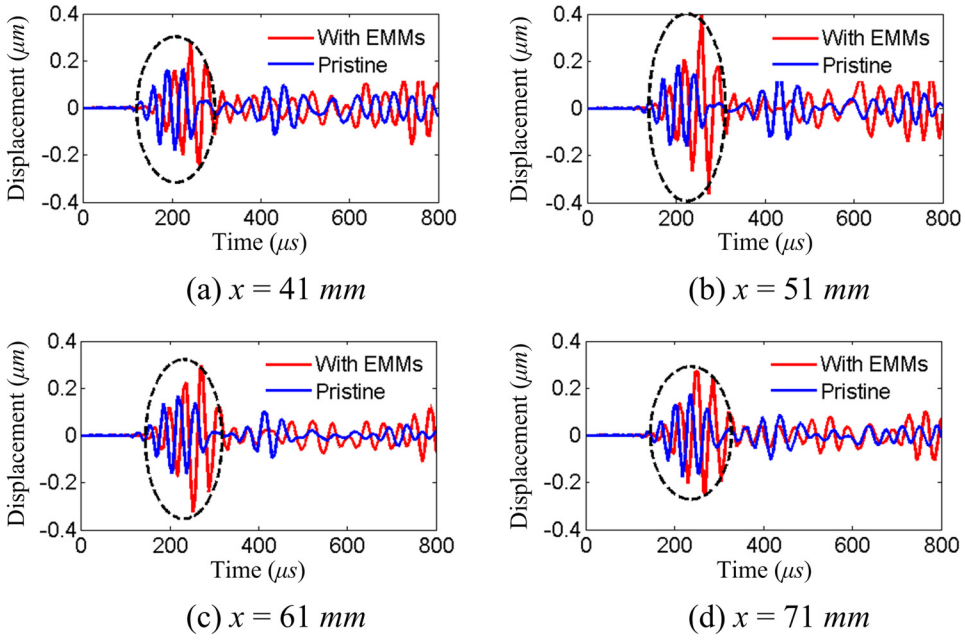

(a) $x = 41\ mm$ (b) $x = 51\ mm$

(c) $x = 61\ mm$ (d) $x = 71\ mm$

FIG. 7. Out-of-plane displacement response beyond EMMs.

region. Figures 7(a)–7(d) show the comparison of displacement response of EMM plate and pristine plate at four different locations. From the figures, the five-peaked waveform still retains with small phase difference after the Lamb waves propagate past through the EMMs region, and the slightly phase difference might be caused by the bending effect which requires more time for waves travelling to those locations. However, with inclusion of EMMs, the amplitude of the Lamb waves has been amplified for each location and the largest amplitude is observed at $x = 51$ mm, which is located around the focal spot area with the amplitude over twice of the same location without EMMs.

In summary, the proposed low-frequency A_0 mode Lamb waves focusing method by simply bonding the EMMs on the plate surface may have good potential in Lamb waves based damage detection for SHM. With EMMs affixed on the host plate, Lamb waves can be manipulated by controlling and focusing the waves to any arbitrary position in the plate where sensors are located, and thus the signal-to-noise ratio would be enhanced greatly with the amplified signal.

The first author would like to thank the financial support from China Scholarship Council in pursuing his Ph.D. dissertation.

[1]R. K. Ing, M. Fink, and O. Casula, Appl. Phys. Lett. **68**(2), 161 (1996).
[2]W. A. K. Deutsch, A. Cheng, and J. D. Achenbach, Res. Nondestruct. Eval. **9**(2), 81 (1997).
[3]R. K. Ing and M. Fink, Ultrasonics **36**, 179 (1998).
[4]T. T. Wu, Y. T. Chen, J. H. Sun, S. C. S. Lin, and T. J. Huang, Appl. Phys. Lett. **98**, 171911 (2011).
[5]J. F. Zhao, R. Marchal, B. Bonello, and O. Boyko, Appl. Phys. Lett. **101**, 261905 (2012).
[6]L. Fok, M. Ambati, and X. Zhang, Mater. Res. Soc. Bull. **33**(10), 931 (2008).
[7]X. M. Zhou, X. N. Liu, and G. K. Hu, Theor. Appl. Mech. Lett. **2**, 041001 (2012).
[8]H. H. Huang, C. T. Sun, and G. L. Huang, Int. J. Eng. Sci. **47**, 610 (2009).

[9]Y. Wu, Y. Lai, and Z. Q. Zhang, Phys. Rev. Lett. **107**, 105506 (2011).
[10]X. N. Liu, G. K. Hu, G. L. Huang, and C. T. Sun, Appl. Phys. Lett. **98**, 251907 (2011).
[11]The material properties are: aluminum: $\rho = 2713\,\mathrm{kg/m^3}$, $E = 72.6\,\mathrm{Gpa}$, $\nu = 0.33$; Silicone rubber: $\rho_r = 1250\,\mathrm{kg/m^3}$, $E_r = 0.01\,\mathrm{Gpa}$, $\nu = 0.499$; Lead: $\rho_l = 11340\,\mathrm{kg/m^3}$, $E_l = 11\,\mathrm{Gpa}$, $\nu = 0.435$.
[12]C. Gomez-Reino, M. V. Perez, and C. Bao, *Gradient-Index Optics: Fundamentals and Applications* (Springer, Berlin, 2002).
[13]S. C. Lin, T. J. Huang, J. H. Sun, and T. T. Wu, Phys. Rev. B **79**, 094302 (2009).
[14]R. Zhu, X. N. Liu, G. L. Huang, H. H. Huang, and C. T. Sun, Phys. Rev. B **86**, 144307 (2012).